Influence of the applied power on the barrier performance of silicon-containing plasma polymer coatings using a hollow cathode-activated PECVD process

Top, Michiel; Fahlteich, John; De Hosson, Jeff T. M.

Published in:
Plasma processes and polymers

DOI:
10.1002/ppap.201700016

Received: 21 January 2017 | Revised: 7 March 2017 | Accepted: 8 March 2017

DOI 10.1002/ppap.201700016

PLASMA PROCESSES AND POLYMERS

FULL PAPER

Influence of the applied power on the barrier performance of silicon-containing plasma polymer coatings using a hollow cathode-activated PECVD process

Michiel Top[1,2] | **John Fahlteich**[1] | **Jeff T. M. De Hosson**[2]

[1] Fraunhofer Institute for Organic Electronics, Electron Beam and Plasma Technology FEP, Dresden, Germany

[2] Department of Applied Physics, University of Groningen, Groningen, The Netherlands

Correspondence
Michiel Top, Fraunhofer Institute for Organic Electronics, Electron Beam and Plasma Technology FEP, Winterbergstrasse 28, 01277 Dresden, Germany.
Email: michiel.top@fep.fraunhofer.de

Funding information
Fraunhofer-Gesellschaft, Grant number: FlexKap

A hollow cathode arc discharge is used for the roll-to-roll deposition of silicon-containing plasma polymer thin films on a polymer substrate. It is found that the fragmentation of the used monomer hexamethyldisiloxane (HMDSO) increases with increasing plasma power. The higher fragmentation was related to a reduced hydrogen content as a result of breaking C─H bonds. This allowed for a higher degree of cross-linking. The latter has a positive effect on the barrier performance of the coatings. A hollow cathode arc discharge with separate anode allowed the deposition of a plasma polymer with a water vapor transmission rate (WVTR) of 0.16 g m^{-2} day^{-1} (measured at 38 °C and 90% r.h.) on a PET substrate while maintaining a deposition rate of approximately 450 nm m min^{-1}.

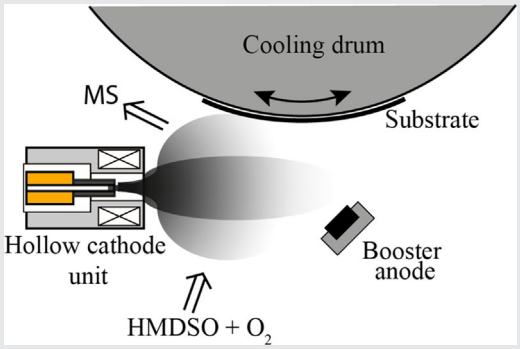

KEYWORDS
barrier, DC discharges, hexamethyldisiloxane (HMDSO), hollow cathode, plasma polymerization

1 | INTRODUCTION

Plasma enhanced chemical vapor deposition (PECVD) is an attractive process that can be used for the deposition of organic plasma polymer and SiO_2-like layers. Deposited films can be used as barrier for water vapor or oxygen,[1,2] as scratch resistance coating[3] or they can be used in optical systems.[4] In previous research,[5] silicon-containing plasma polymer films that were deposited using a dynamic hollow cathode arc discharge PECVD process showed a water vapor transmission rates (WVTR) of 0.16 g m^{-2} day^{-1} (measured at 38 °C and 90% r.h.). While the change of oxygen to HMDSO ratio showed a clear correlation with the chemical and optical properties, no explanation was found for the change in barrier performance.

Considerable literature is already available on the relation between the plasma process parameters and the barrier performance. The influence of the ratio between oxygen and the monomer flow,[6–8] substrate bias,[6] substrate temperature[9], and plasma power input[7,10–12] were already investigated for selected types of plasma. Relevant work was done by Creatore et al.[13,14] on the identification of critical precursors for barrier coatings using high power and highly diluted HMDSO depositions using a RF plasma. Zhang et al.[15] showed that the oxygen transmission rate of organic coatings depends on the electrical frequency of the plasma. In contrast to the literature, this paper will discuss the

influence of the applied plasma current and power of a DC hollow cathode arc discharge on the barrier performance of highly organic coatings.

The high electron density of the hollow cathode as well as the high energy low voltage electron beam[16] show potential for efficient ionization and dissociation of the applied monomer and reactive gas, i.e., for the high-rate deposition of high-quality films. Several researchers already investigated the deposition of plasma polymers using a hollow cathode.[17–19] This paper sets aside of the previous approaches because they used an RF power supplies without an additional booster anode. Second, no WVTR values are given in literature. In this paper, we employ mass spectrometry and several thin film analysis methods and propose a complete step-by-step analysis of the relation between the process parameters and the barrier performance of the deposited thin films.

2 | EXPERIMENTAL SETUP

The hollow cathodes and booster anodes in the *novoFlex® 600* were used for the deposition of silicon-containing plasma polymer films. General information about the roll-to-roll web coater has been described elsewhere.[4] A schematic representation of the PECVD chamber is shown in Figure 1. To the left, the hollow cathode unit is located which is equipped with a molybdenum cylinder that functions as cathode and an annular graphite ring being the anode. Argon is purged through the cathode and anode. An additional coil is wound at the right side of the unit which can be used to generate an axial magnetic field. The booster anode is made of graphite and is mounted in a copper mount. Both the hollow cathodes and booster anodes are operated in DC-mode using a current driven power supply. These systems uses a feedback loop that regulates the voltage in order to keep the current constant. Therefore, in this specific setup, the plasma resistivity has a direct effect on the applied voltage and therefore the applied power.

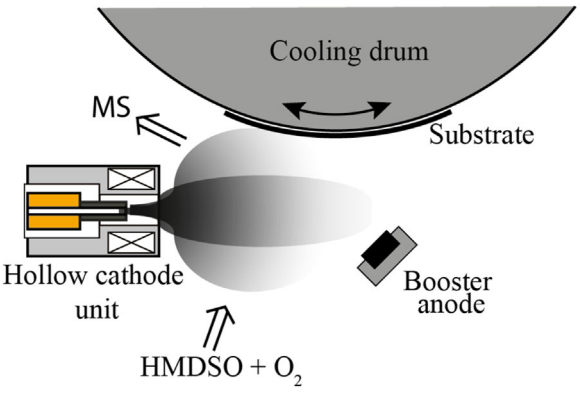

FIGURE 1 A schematic representation of the hollow cathode PECVD deposition geometry

Several parameters are available to change systematically the plasma resistivity, i.e., allowing a change in the applied power without changing the applied current. Since the plasma resistivity directly depends on the collision frequency,[20] it can be influenced by process parameters which have a direct effect on the particle density. The two effective methods to decrease the particle density are the reduction of the process gas flow and the reduction of the axial magnetic field. The latter influences the electron distribution between the hollow cathode and separate booster anode[21] and therefore influences the electrical properties of the plasma.

The coatings were produced at a constant oxygen to HMDSO ratio, equal to two. The HMDSO flow was varied between 125 and 1000 sccm for the mass spectrometry analysis but was fixed at 125 sccm for the thin film analysis. The substrate was a PET polymer film (Melinex 401 CW, 75 µm thickness) with 650 mm width. Unless mentioned otherwise, the web speed was set at 1 m min^{-1}. The analyzed samples were taken out of the center of the substrate. Booster anode current, axial magnetic field (varied by modification of an electric coil current between 4 and 10 A), and the argon flow in the reaction chamber (250–500 sccm) were varied to obtain changes in the plasma resistivity. The cooling drum was actively cooled to remain at a constant temperature of 0 °C. During the deposition, both the applied electrical current and voltage were measured. In the following, the current and power are referred to as I and P with subscripts BA and AA for booster anode and annular anode, respectively. To allow a comparison with other deposition systems, the power will be given as W per sccm of HMDSO. This is in accordance to the Yasuda factor[22] which describes that the applied power divided by the product of the monomer mass and flow is an important quantity for the comparison between different PECVD processes.

To analyze the plasma, a QMG 220 Mass Spectrometer from Pfeiffer Vacuum was connected to the reaction chamber. The mass spectrometer analyzes fragments with a mass between 1 and 100 amu. At least five spectra were taken for each sample and the average spectrum was used for the evaluation.

After deposition, the WVTR was measured at 38 °C and 90% r.h. using a coulometric water vapor permeability tester (WDDG, Brugger Feinmechanik). The effective measurement area was approximately 80 cm^2. The chemical composition was analyzed using X-ray photoelectron spectroscopy (XPS) and glow-discharge optical emission spectroscopy (GD-OES). Before performing the XPS measurements, 20 nm was etched away using an argon plasma (4 keV) to remove surface contamination. After etching, XPS measurements were performed using a 12 kV Mg-kα X-ray beam and a Phoibos 100 MCD hemispherical analyzer. Afterwards, a quantitative evaluation of the silicon, carbon, and oxygen content was

executed. Because Rzeznik et al.[23] showed that preferential sputtering influences the calculation of the composition after ion bombardment with argon atoms with energies up to 30 keV, XPS measurements were performed at 10 and 20 nm depth for one of the samples to check whether preferential sputtering influenced the measurements. A slight decrease of carbon and a slight increase of oxygen were observed. However, all within ±3 at%. This indicates that preferential sputtering can be neglected here and that the pre-cleaning step does not falsify the results.

GD-OES measurements were performed using a GD Profiler 2 (Horiba Scientific) in RF Plasma mode with argon as a process gas. The plasma was additionally pulsed to minimize the thermal load on the samples. The transition from coating to substrate was derived from the silicon signal reaching to zero in the substrate. The top and bottom part of the coating were taken out of the quantitative analysis to avoid interface and surface absorption and diffusion effects. The middle part was used to calculate the average hydrogen, silicon, carbon, and oxygen signals. Quantitative GD-OES analysis was not possible because the hydrogen is known to influence the emission spectra.[24] However, the intensity of the hydrogen line was analyzed to give a qualitative estimation of the hydrogen content. The normalized hydrogen content was calculated by

$$\frac{\int H\ [V]}{\int H\ [V] + \int C\ [V] + \int O\ [V] + \int \mathrm{Si}\ [V]} \quad (1)$$

In this equation, $\int X\ [V]$ represents the averaged signal in the bulk of the coating of element X.

The chemical bonds in the samples were analyzed using attenuated total reflectance Fourier transformed infrared (ATR-FTIR) spectroscopy. A Spectrum 2000 (Perkin Elmer) FTIR spectrometer was used. An ATR add-on with a germanium crystal was employed to limit the penetration depth between approximately 760 and 1260 nm for the analyzed domain. Since the thin films were usually smaller, it should be realized that part of the PET substrate is also measured.

X-ray reflectometry (Bruker Discover D8) was applied to estimate the mass density of the deposited films by measuring the X-ray reflection between 0 and 2°. The measurement curves were fitted using the Gen-X software.[25] The XPS data were used for the conversion of the electron density into the mass density. The error due to the lack of quantitative hydrogen data was described in previous research.[5]

3 | RESULTS

Multiple samples were produced with a constant I_{BA} of 2.4 A sccm^{-1} HMDSO. The pressure in the chamber was measured between 0.07 and 0.1 Pa during the experiments.

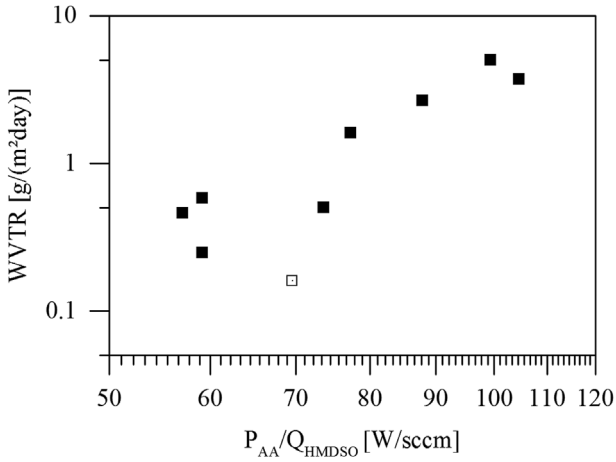

FIGURE 2 The WVTR (at 38 °C and 90% r.h.) of the thin films coatings is plotted as a function of the applied power per unit of monomer between the hollow cathode and the annular anode (P_{AA})

The applied voltage was varied using different parameters as described in the experimental part. WVTR's were measured between 0.16 and 6.3 g m^{-2} day^{-1}. This shows that there is no correlation between the applied current and the barrier performance. To analyze the relation between functional properties and the applied power, the barrier performance was also plotted as a function of P_{AA} and P_{BA}. These results are shown in Figures 2 and 3, respectively. The vertical axis shows the Water Vapor Transmission Rate in g m^{-2} day^{-1} (measured at 38 °C and 90% r.h.) whereas the horizontal axis shows the applied power divided by the monomer flow.

An inverse relation was found between P_{AA} and the barrier performance of the coatings whereas a direct correlation was found between the barrier performance and P_{BA}. The measured power between the hollow cathode and the annular anode mostly represents the plasma directly around the hollow cathode unit and the P_{BA} directly applies to

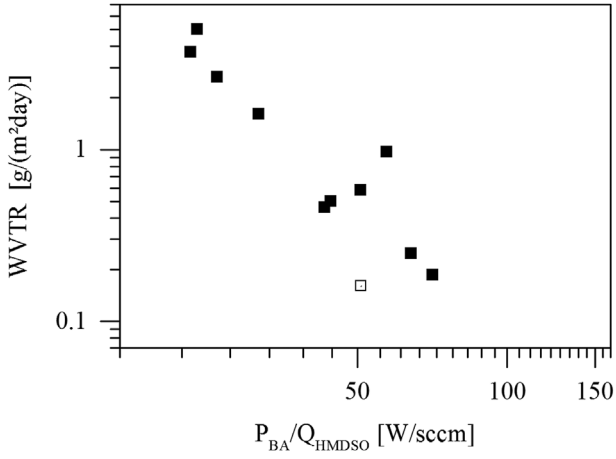

FIGURE 3 The WVTR (at 38 °C and 90% r.h.) of the thin films coatings is plotted as a function of applied power per unit of monomer at the booster anode (P_{BA})

the applied power in the reaction chamber and therefore describes the plasma that directly influences the fragmentation and ionization of the monomer and reactive gas before deposition. The direct relation between P_{BA} and the barrier indicates that the dissociation of the monomer plays a predominant role.

As the film thickness of the coating usually plays an important role in the barrier performance, the coating thicknesses were analyzed. All coatings have a thickness between 330 and 510 nm. As all samples were deposited at 1 m min^{-1}, this also indicates that the power influences the deposition rate. A tendency is shown that for higher coating thicknesses, the barrier improves. However, for selected samples, a thickness increase of 20% shows a barrier improvement from 4 down to 0.25 g m^{-2} day. It is also observed that the sample with the highest thickness (520 nm) shows hardly any improved barrier performance. The higher thickness could be a result of a more porous structure which again leads to the lack of barrier.

To obtain a clear relation between the barrier performance and the barrier film thickness, several samples were made while keeping the plasma constant while changing the web speed. The result is shown in Figure 4. Up to 150 nm film thickness, a steady decrease of the WVTR is observed. However, above this thickness, only slight improvements are observed. As all the film thicknesses investigated within this paper were between 350 and 510 nm, no changes in the barrier performance are expected as a result of the WVTR. This clearly indicates that the barrier performance was not influenced by the coating thickness.

3.1 | Fragmentation of HMDSO

Mass spectrometry showed a variety of peaks between 1 and 100 atomic mass units (amu) which can be assigned to HMDSO fragments and the process and reactive gas. Figure 5 shows a spectrum from one of the samples where selected peaks are assigned. The spectrum was taken at a low power per sccm HMDSO to make the peaks above 50 amu clearly visible. For the evaluation of the spectra, the observed peaks were divided into two groups with masses below and above 50 amu as indicated by the dotted line. The first group is assigned to single molecules and small groups (e.g., O_2, argon, C, H_2O, Si^+) which are a result of oxidation reactions and hydrocarbon chemistry.[26] The latter group represents larger fragments which can be assigned to intermediate products of the HMDSO molecule as described in literature.[27] In our spectra, peaks were found for $SiOC_2H_8$, $SiO(CH_3)$, $Si_2O(CH_3)_4$, $Si(CH_3)_4$), and Si_2OH. As a measure of the dissociation of the HMDSO molecule, the sum of the peaks of the fragments with masses below 50 amu were divided by the sum of the peaks above 50 amu.

The dissociation was found to correlate with the following parameters:

$$\frac{A_{<50}}{A_{>50}} \propto \left(\frac{P_{BA}}{Q_{HMDSO}}\right)^{\alpha} \times Q_{BA,Ar} \times Q_{O_2} \quad (2)$$

In this equation, P_{BA} represents the Booster Anode Power, Q represents the flows of HMDSO, the argon through the booster anode and oxygen. The measured dissociation was plotted against Equation (2) in Figure 6.

The first part of Equation (2) represents the applied power per unit of monomer which is consistent with the findings by Yasuda.[22] The influence of the fragmentation of oxygen was also observed by Li.[28] The increase of argon results in a higher pressure, which increases the collision rate and therefore is thought to have a positive effect on the dissociation of the HMDSO. The value for α was chosen

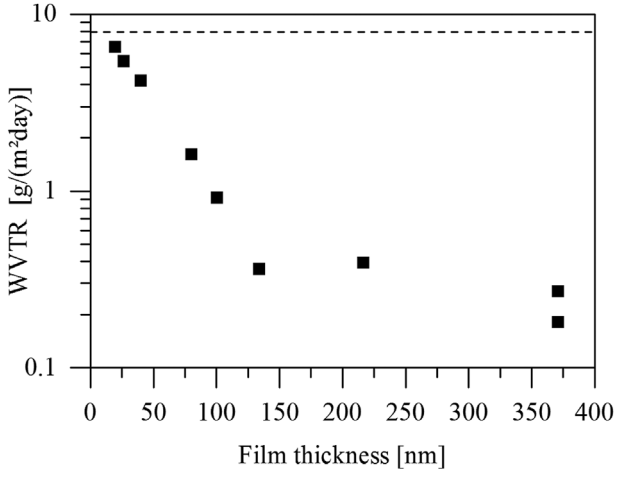

FIGURE 4 The WVTR (measured at 38 °C and 90% r.h.) of the coated films was plotted as a function of the film thickness. The thickness was varied by changing the web speed of the substrate. The dashed line indicates the WVTR of the bare PET substrate

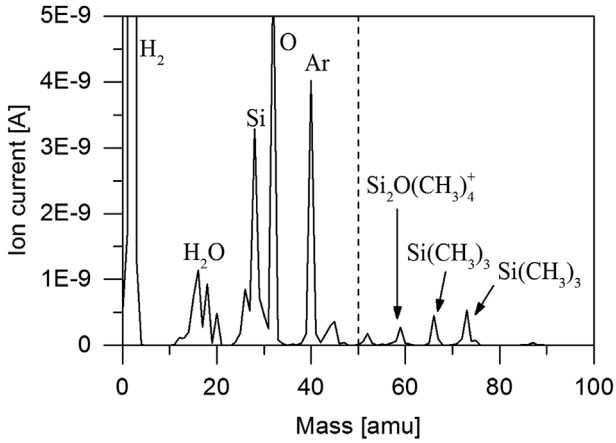

FIGURE 5 A typical mass spectrum for a deposition with a low power per unit of monomer. Peaks at the left part of the dashed line are mainly assigned to single atoms or small molecules. The peaks at the right side could be assigned to larger fragments of the HMDSO molecule. The main peaks are identified in the figure

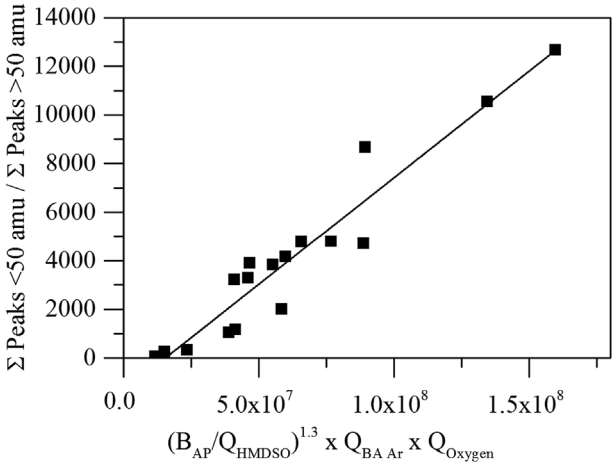

FIGURE 6 The degree of fragmentation was analyzed taking the ratio between the sum of the peaks below 50 amu and the sum of the peaks above 50 amu. The dissociation was plotted as a function of several process parameters as shown in Equation (2)

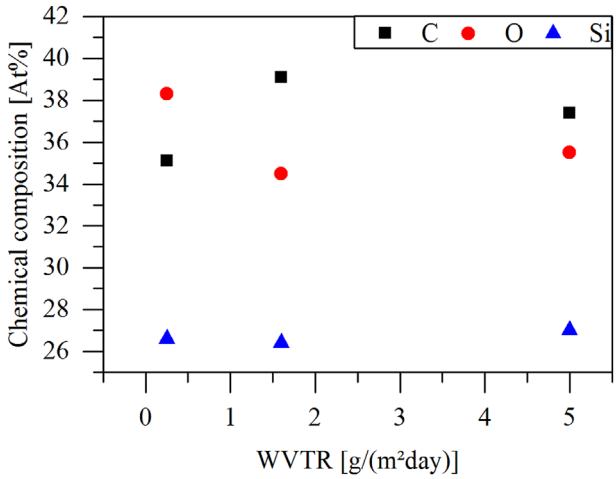

FIGURE 7 The relative chemical composition of carbon, oxygen, and silicon at a depth of 20 nm as measured by XPS shown for three samples with WVTR's between 0.1 and 5 g/(m^{2}day)

such that the R-square value between the fit and the data points was maximized. This maxima was found at $\alpha = 1.3$. This indicates that the power per unit of monomer has a higher influence on the dissociation compared to the argon and oxygen flow.

3.2 | Thin film analysis

So far it was shown that the increased P_{BA} results in a higher dissociation of the monomer. The deposited films were analyzed to evaluate how the increased dissociation results in a better barrier performance. The thin film analysis was limited to the samples with an HMDSO flow of 125 sccm. For higher flows, the plasma power per unit of monomer was found to be not sufficient to improve significantly the barrier performance of the PET substrate. Further reduction of the monomer flow as well as further increase of the applied power was not possible because the heat transfer from the plasma into the substrate exceeded the critical thermal load of the polymer substrate.

The plasma analysis shows that the fragmentation of the HMDSO monomer increases with the applied power. XPS was used to measure the atomic weight of Si, O, and C for selected samples with a WVTR between 0.16 and 5 g m^{-2} day^{-1}. All samples showed a composition with a Si:O:C contribution of 27:36:37 (±2) at%. No correlation between the chemical composition and the WVTR was found, as shown in Figure 7. The measured variation is therefore related to the measurement error as well as statistical variation. This indicates there is no significant shift in the chemical composition from organic to inorganic with increasing power. Because the XPS measurement showed no changes, the relative change in hydrogen content was measured using GD-OES. The WVTR was plotted as a function of the measured normalized hydrogen content in Figure 8. It is seen that the hydrogen content increases with increasing WVTR. One specimen which did not follow the trend is the specimen with a hydrogen signal of 0.413 V (open square). Even though it has the highest hydrogen content it shows a very low WVTR. This sample will be discussed later on.

It was described in literature that a higher mass density usually leads to an improved barrier performance.[7,12] This relation was checked by measuring the mass density of the coatings. Figure 9 shows the relation between the mass density and the WVTR. Even though there is no perfect correlation, an increased mass density indicates an improved barrier performance. It should be mentioned that the density calculation depends on the chemical composition of the thin film. For the calculation of the mass density, the hydrogen content is not taken into account. This leads to an

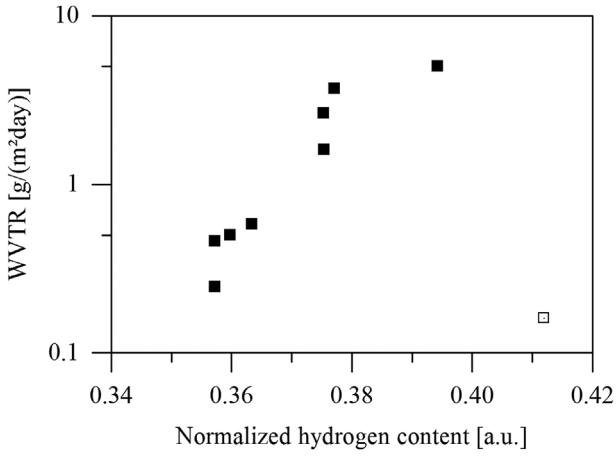

FIGURE 8 The WVTR (measured at 38 °C and 90% r.h.) of the thin films coatings plotted as a function of the normalized hydrogen content (Equation 1) measured by GD-OES

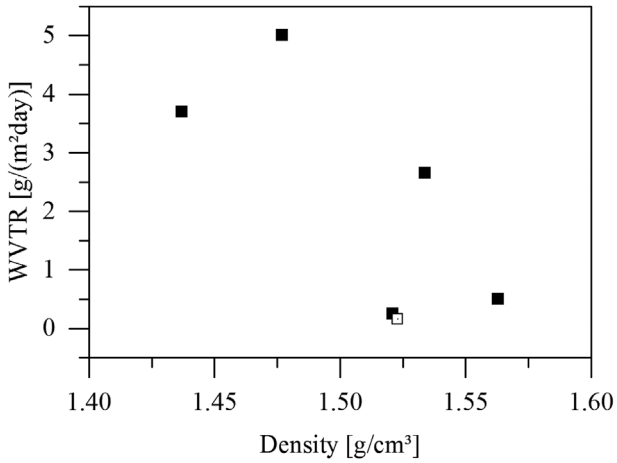

FIGURE 9 The WVTR (measured at 38 °C and 90% r.h.) of the thin films coatings plotted as a function of the thin film density measured using XRR

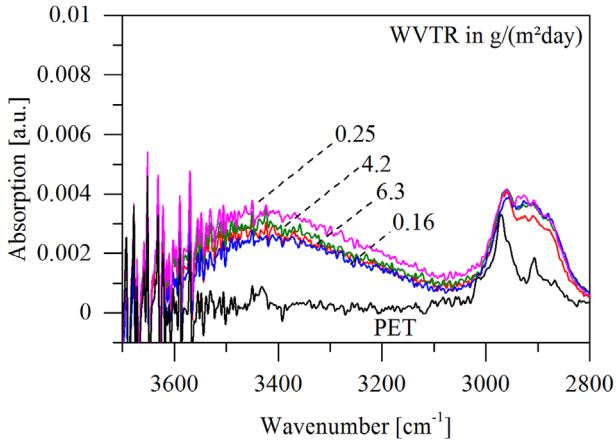

FIGURE 10 IR-ATR spectra between 2800 and 3700 cm^{-1} of several SiOx samples with WVTR's between 6.3 and 0.16 g/m^2day. The black line represents the spectra of bare PET

overestimation of the calculated density (up to 0.08 g cm^{-3}). However, a reduction of the hydrogen content reduces the overestimation of the density. Therefore, the actual increase of the mass density with applied power could be even larger. From the GD-OES and XRR results, it can be concluded that the lower hydrogen content increases the thin film density. The hydrogen reduction allows more cross-linking within the coating. The more dense packed molecules would result in a higher density of the film.

Our analysis up to this point shows that the increased power results in higher fragmentation of the monomer and that less hydrogen present in the deposited films improves the barrier performance. This reduction could be assigned to the reduction of Si—H, O—H, and C—H bonds in the coating. ATR-FTIR was used to analyze the influence from each of these three bonds.

Figure 10 shows the IR-ATR spectra for selected samples with the measured water vapor barrier rates between 0.16 and 6.3 g m^{-2} day^{-1}. Unless stated otherwise, the other samples showed similar behavior. The numbers shown in the figure correspond to the measured WVTR of the samples. For the coated films, a broad peak is observed between 3000 and 3500 cm^{-1} which is assigned to the presence of O—H bonds.[29] The black line represents the bare PET which shows no significant increase between 3000 and 3500 cm^{-1}. Therefore, the influence of the substrate can be ignored in this domain. The discrepancy between the lines lies within the measurement error bars and no correlation has been found between the WVTR and a change in the number of OH bonds. Figure 10 also shows the peaks from 2800 till 3000 cm^{-1}. These are assigned to the C—H stretching within CH_x groups.[19,30] These peaks are to a large extent overlapped by the PET structure. Even though it is clear that the coating still obtains C—H bonds, no conclusions can be drawn regarding the change of these bonds in a quantitative sense.

The domain between 2260 and 2095 cm^{-1} was analyzed for the presence of Si—H bonds.[29] Figure 11 shows this domain for the same samples as shown in Figure 10. The black line again represents the bare PET. Also in this domain, the PET does not influence the measured intensity. The numbers shown in the graph denote the measured WVTR. Some spread was found between the different samples. However, no correlation was found between the presence of Si—H bonds and the barrier performance. Therefore it is thought that the deviations are due to insignificant statistical variations in the coatings.

As a result, the reduction of water content should probably be assigned to breaking of Si—C and/or C—H bonds. The characterization of these bonds, which lies in the domain between 900 and 1500 cm^{-1}, was difficult because the C—H bonds which are present in the PET are interfering with the spectra of the samples. However, a significant increase of a broad peak between 1000 and 1060 cm^{-1} was observed for lower water diffusion rates. This peak is related to various

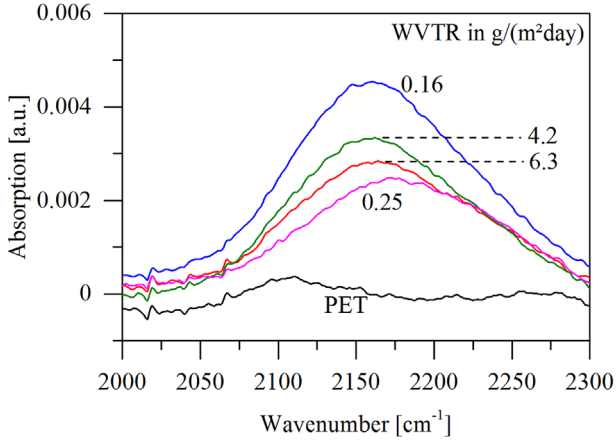

FIGURE 11 IR-ATR between 2000 and 2300 cm^{-1} spectra of several SiOx samples with WVTR's between 6.3 and 0.16 g/m^2day. The black line represents the spectra of bare PET

Si—O—Si and Si—O—C bond and stretching modes.[19,30–32] Therefore, it is most likely that the increased plasma power results in the breaking of C—H bonds in the HMDSO molecule. As a result, the Si—O—Si and Si—O—C bonds are not terminated by hydrogen groups, which allows a higher degree of crosslinking and the formation of a more dense structure improving the barrier performance. Similar relations between the plasma power and the degree of cross-linking have been found for other types of plasma polymer films.[33–35]

This explanation is consistent with the fragmentation of HMDSO as described in literature. [26,27,30] The first dissociation steps are the removal of CH_3 groups and the breaking of Si—C bonds. The remaining Si-$(CH_x)_x$ groups are incorporated in the film. At higher power, these fragments are fragmentized and the hydrogen may react, e.g., with oxygen and is pumped away as H_2O. The reduction of hydrogen and CH_3 groups allows for a higher degree of cross-linking and therefore increases the density of the film.

4 | DISCUSSION

The samples discussed in this paper were made during different deposition runs to make sure that reproduction was possible. Almost all samples are in good agreement with the proposed mechanism for improved barrier performance. One sample, however, deviates from this trend. This sample was indicated throughout the paper with an open square. The sample with a low WVTR of 0.16 $g\,m^{-2}\,day^{-1}$ shows good performance, however, it shows a high hydrogen signal as well as a slightly higher Si—H signal. So far, no clear explanation has been found for this specimen. Reproduction of this specific sample has not been possible up to this point.

During the analysis of the thin film properties, no correlation was found between barrier performance and the applied current. Because the same current was applied to the booster anode for most of the analyzed coatings, it could be argued whether the barrier performance depends on the booster anode voltage or power. Applying multiple currents while keeping the power constant leads to drastic differences in the deposition rate making a comparison between the coatings more difficult. Even so, changing the applied current influences the voltage. Since the plasma analysis, which was measured for a wide variety of applied currents, voltages, and powers, showed a good relation between the defragmentation and the applied power, this seems to be the critical parameter.

5 | CONCLUSION

This paper concentrates on the influence of electrical parameters of a hollow cathode-activated plasma with a separate booster anode on the water vapor barrier performance of the deposited silicon-containing plasma polymer thin films. A step-by-step explanation was given of the relation between the applied plasma power and barrier performance for organic plasma polymer films.

The improved barrier performance is due to the increased density of the deposited plasma polymer film. The higher density was found to be a result of the reduced hydrogen content in the films. Since the IR-ATR analysis showed no correlation between the barrier performance and the O—H or Si—H bonds, the reduced hydrogen should be a result of the breaking of C—H bonds. Therefore, sufficient power is necessary to break C—H bonds in the HMDSO molecule allowing for the formation of sufficiently dense coatings that exhibit a low WVTR.

ACKNOWLEDGEMENTS

These results presented in this work were funded by the Fraunhofer project “flexKap.” The authors thank Dr. O. Zywitzki and his coworkers of the Materials Analysis Department at Fraunhofer FEP for the GD-OES and permeation measurements. Thanks also go to the group of Prof. Dr. C. Reinhold at the FH Zwickau for their help with the XRR measurements on flexible substrates and Dr. E. Langer of the TU Dresden for the XPS measurements.

REFERENCES

[1] M. Komada, T. Oboshi, K. Ichimura, in Proceedings of the 43th Annual Technical Conference of the Society of Vacuum Coaters, United States, **2000**, 352.

[2] J. Madocks, J. Rewhinkle, L. Barton, *Mater. Sci. Eng. B* **2005**, *119*, 268.

[3] B. Bhushan, *Fundamentals of Tribology and Bridging the Gap Between the Macro- and Micro/Nanoscales*, Springer, Dordrecht, Netherlands **2001**.

[4] S. Günther, M. Fahland, J. Fahlteich, B. Meyer, S. Straach, N. Schiller, *Thin Solid Films* **2013**, *532*, 44.

[5] M. Top, S. Schönfeld, J. Fahlteich, S. Bunk, T. Kühnel, S. Straach, J. T. de Hosson, *Surf. Coat. Technol.* **2016**, *314*, 155–159.

[6] S. Steves, B. Ozkaya, C-N Liu, O. Ozcan, N. Bibinov, G. Grundmeier, P. Awakowicz, *J. Phys. D: Appl. Phys.* **2013**, *46*, 84013.

[7] A. Bieder, A. Gruniger, R. von Rohr, *Surf. Coat. Technol.* **2005**, *200*, 928.

[8] J. Fahlteich, Transparente Hochbarriereschichten auf flexiblen Substraten, PhD Thesis, **2010**, Chemnitz.

[9] D. S. Wuu, W. C. Lo, C. C. Chiang, H. B. Lin, L. S. Chang, R. H. Horng, C. L. Huang, Y. J. Gao, *Surf. Coat. Technol.* **2005**, *197*, 253.

[10] A. W. Smith, N. Copeland, D. Gerrerd, D. Nicholas, in 34th Annual Technical Conference proceedings of the Society of Vacuum Coaters **1991**, 525.

[11] A. G. Erlat, R. J. Spontak, R. P. Clarke, T. C. Robinson, P. D. Haaland, Y. Tropsha, N. G. Harvey, E. A. Vogler, *J. Phys. Chem. B* **1999**, *103*, 6047.

[12] D. S. Wuu, W. C. Lo, L. S. Chang, R. H. Horng, *Thin Solid Films* **2004**, *468*, 105.

[13] M. Creatore, F. Palumbo, R. D'Agostino, *Plasmas Polym.* **2002**, *7*, 291.

[14] M. Creatore, F. Palumbo, R. D'Agostino, P. Fayet, *Surf. Coat. Technol.* **2001**, *142–144*, 163.

[15] J. Zhang, Q. Chen, Y. Zhang, F. Liu, Z. Liu, The proceedings of the 1st International Conference on Microelectronics and Plasma Technology (ICMAP 2008) **2009**, *517*, 3850.

[16] H. Morgner, M. Neumann, S. Straach, M. Krug, *Surf. Coat. Technol.* **1998**, *108–109*, 513.

[17] C. L. Fan, P. C. Chiu, Y. H. Yang, C. C. Lin, *Semicond. Sci. Tech.* **2010**, *25*, 75006.

[18] F. Jansen, S. Krommenhoek, *Thin Solid Films* **1994**, *252*, 32.

[19] S. Saloum, M. Naddaf, B. Alkhaled, *Vacuum* **2008**, *82*, 742.

[20] W. Baumjohann, R. A. Treumann, *Basic Space Plasma Physics*, Imperial College Press; distributed by World Scientific Pub., London, River Edge, N.J. **1997**.

[21] F. Fietzke, H. Morgner, S. Günther, *Plasma Process. Polym.* **2009**, *6*, 242.

[22] H. Yasuda, *Plasma Polymerization*, Academic Press, Orlando **1985**.

[23] L. Rzeznik, Y. Fleming, T. Wirtz, P. Philipp, *Beilstein J. Nanotechnol.* **2016**, *7*, 1113.

[24] J. Angeli, A. Bengtson, A. Bogaerts, V. Hoffmann, V.-D. Hodoroaba, E. Steers, *J. Anal. At. Spectrom.* **2003**, *18*, 670.

[25] M. Björck, G. Andersson, *J. Appl. Crystallogr.* **2007**, *40*, 1174.

[26] D. Magni, C. Deschenaux, C. Hollenstein, A. Creatore, P. Fayet, *J. Phys. D: Appl. Phys.* **2001**, *34*, 87.

[27] R. Basner, R. Foest, M. Schmidt, K. Becker, H. Deutsch, *Int. J. Mass Spectrom.* **1998**, *176*, 245.

[28] K. Li, O. Gabriel, J. Meichsner, *J. Phys. D: Appl. Phys.* **2004**, *37*, 588.

[29] S. Holly, P. Sohár, L. Láng, *Absorption Spectra in the Infrared Region*, Akadémiai Kiadó, Budapest **1977**.

[30] M. T. Kim, *Thin Solid Films* **1997**, *311*, 157.

[31] D. S. Wavhal, J. Zhang, M. L. Steen, E. R. Fisher, *Plasma Process. Polym.* **2006**, *3*, 276.

[32] Y. B. Park, S. W. Rhee, *J. Appl. Phys.* **1999**, *86*, 1346.

[33] S. Ligot, E. Bousser, D. Cossement, J. Klemberg-Sapieha, P. Viville, P. Dubois, R. Snyders, *Plasma Process. Polym.* **2015**, *12*, 508.

[34] D. Hegemann, E. Körner, N. Blanchard, M. Drabik, S. Guimond, *Appl. Phys. Lett.* **2012**, *101*, 211603.

[35] L. Denis, F. Renaux, D. Cossement, C. Bittencourt, N. Tuccitto, A. Licciardello, M. Hecq, R. Snyders, *Plasma Process. Polym.* **2011**, *8*, 127.

How to cite this article: Top M, Fahlteich J, De Hosson JTM. Influence of the applied power on the barrier performance of silicon-containing plasma polymer coatings using a hollow cathode-activated PECVD process. *Plasma Process Polym.* 2017;14: e1700016. https://doi.org/10.1002/ppap.201700016